Communication

Dynamic in Situ Electrochemical Neutron Reflectivity Measurements

Jonathan M. Cooper, Robert Cubitt, Robert M. Dalgliesh, Nikolaj Gadegaard, Andrew Glidle, A. Robert Hillman, Roger J. Mortimer, Karl S. Ryder, and Emma L. Smith

J. Am. Chem. Soc., **2004**, 126 (47), 15362-15363• DOI: 10.1021/ja044682s • Publication Date (Web): 06 November 2004

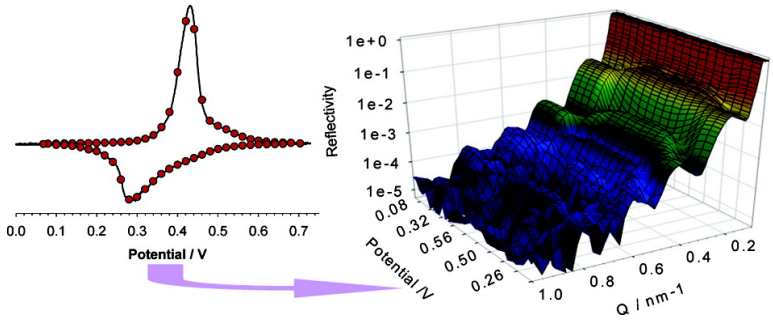

More About This Article

Additional resources and features associated with this article are available within the HTML version:

- Supporting Information
- Links to the 3 articles that cite this article, as of the time of this article download
- Access to high resolution figures
- Links to articles and content related to this article
- Copyright permission to reproduce figures and/or text from this article

View the Full Text HTML

J|A|C|S
COMMUNICATIONS

Published on Web 11/06/2004

Dynamic in Situ Electrochemical Neutron Reflectivity Measurements

Jonathan M. Cooper,[†] Robert Cubitt,[‡] Robert M. Dalgliesh,[§] Nikolaj Gadegaard,[†] Andrew Glidle,[†] A. Robert Hillman,[*,¶] Roger J. Mortimer,[#] Karl S. Ryder,[¶,#] and Emma L. Smith[#]

Department of Electronics, University of Glasgow, Glasgow, G12 8LT, U.K., Institut Laue Langevin, 38042 Grenoble Cedex 9, France, ISIS Facility, Rutherford Appleton Laboratory, Didcot, OX11 0QX, U.K., Department of Chemistry, University of Leicester, Leicester, LE1 7RH, U.K., and Department of Chemistry, Loughborough University, Loughborough LE11 3TU, U.K.

Received September 2, 2004; E-mail: arh7@le.ac.uk

We report the first dynamic in situ electrochemical neutron reflectivity measurements on electroactive films. The improved time resolution yields individual species profiles at buried interfaces subject to time-variant electrochemical control, providing new insights into transient population distributions.

Assembly of controlled interfacial architecture is a primary goal of interfacial electrochemistry. A generic issue is the extent to which the real interfacial structure and composition correspond to the design. A vast array of surface-sensitive spectroscopic,[1] imaging,[2] electrical,[3] chemical,[4] and acoustic[5] probes have been coupled with electrochemistry to characterize the structure, composition, and dynamics of modified electrodes as functions of time and space. An underexplored aspect is the spatial distribution of species at the interface, which may have greater impact on properties than chemical composition.[6] Generally, spectroscopic measurements give spatially integrated signals. Imaging methods[2] provide lateral mapping of the exterior surface of a film but do not explore the interior, where most of the functionality lies. Ellipsometry[7] can provide internal composition, but despite superb temporal resolution, it is limited by insufficient measurands to ensure unique fits to complex interfacial structures.

A recent technique for characterizing "wet" interfaces is neutron reflectivity[8] (NR). It has many parallels with its optical counterpart, ellipsometry, but with the additional feature of isotopic sensitivity. This "contrast variation" allows one to alter the "visibility" of a selected species. Commonly, the technique exploits H/D substitution, for which the effect is large; we use H_2O/D_2O switching to locate the solvent.

Development of NR to study "buried" interfaces under potential control has distinguished composite and bilayer polymer films,[9] revealed permeating solvent in electroactive polymer[10] and metal hydroxide[11] films, identified permselectivity failure at high electrolyte concentration,[12] and revealed 1D profiling of diffusion and reaction within a film of a solution phase mediator.[13] These and related[14] NR studies have data acquisition time scales of 1−2 h, so one can observe equilibrated films as a function of potential (charge) but not the dynamics of interconversion.

The generic objective is simultaneous spatial and temporal resolution of individual components (polymer, solvent, and ions) within film interiors. For the polyvinylferrocene (PVF) system studied here, this requires NR data leading to counteranion and solvent population changes as functions of time and distance within a redox switching film on a time scale of seconds. This demands an improvement in time resolution of 2−3 orders of magnitude.[8−14] There is no prospect of accomplishing this via an increase in incident flux or detector efficiency. We use a different strategy, boxcar integration within continuous multiple linear potential cycles, to yield the first dynamic in situ electrochemical NR measurements, with an effective time scale of ca. 2 s.

Spin-coated PVF films on 20 nm Au working electrode films (on polished quartz blocks[12,13]) were exposed to aqueous $NaClO_4$ in a three-electrode cell. NR profiles, $R(Q)$, were obtained during voltammetric cycling (at scan rates, $\upsilon = 1$, 5, and 10 mV s^{-1}) using the CRISP and D17 reflectometers at the ISIS Facility and Institut Laue Langevin, respectively. NR data acquired over multiple cycles were sequentially stored in bins associated with 20 mV potential (E) windows and are presented here as a function of momentum transfer, Q (in nm^{-1}) $= (4\pi/\lambda) \sin\theta$, in each potential window accumulated over multiple cycles. At a sweep rate υ (mV s^{-1}), the effective time resolution in seconds is $20/\upsilon$.

Figure 1 shows E- (t-) resolved $R(Q)$ profiles for two films of different surface coverage and at different scan rates to accentuate the effective time-scale differences. End views of the final profiles ($R-Q$ projections) show the familiar pattern of fringes superimposed on the Q^{-4} (Fresnel law) decay. The signal quality is clearly adequate to discern fringes of different periodicity, representing the Au electrode and PVF film thicknesses. Thus, the immediate goal of the study is accomplished; we can acquire high quality NR profiles in situ for electroactive films subject to a time-variant electrochemical control function. Subsequent discussion relates to what can be learned from these results.

To determine *relative* ion and solvent transfer rates *during* redox switching requires comparison of the present data with static[12] NR responses. In H_2O, the relative increases in solvent and ClO_4^- populations accompanying film oxidation are such that their opposing contributions to the total film scattering length density roughly cancel. Long time-scale NR experiments are thus virtually blind to *absolute* solvent and counterion film population changes. However, transient *differential* excursions of the *relative* populations from this compensatory stoichiometry are highlighted. Conversely, the positive scattering lengths of D_2O and ClO_4^- reinforce each other, so experiments in D_2O are optimal for following *integrated* population changes.

The first quantitative outcome is the variation with E of film thickness (h); for a single film, $h = 2\pi/\Delta Q$ (ΔQ = fringe periodicity). Figure 1 is more complex due to the superposition of fringes for the polymer film and the metal electrode. Features due to the PVF layer are most apparent at low Q (<0.6 nm^{-1}). At higher Q, film roughness effects[12] dampen the PVF contributions to the reflectivity, and fringes due to the underlying metal electrode dominate the profile. Variations in the fringe pattern with E are readily seen via the position of the first minimum in $R(Q)$. Film

[†] University of Glasgow.
[‡] Institut Laue Langevin.
[§] Rutherford Appleton Laboratory.
[¶] University of Leicester.
[#] Loughborough University.

10.1021/ja044682s CCC: $27.50

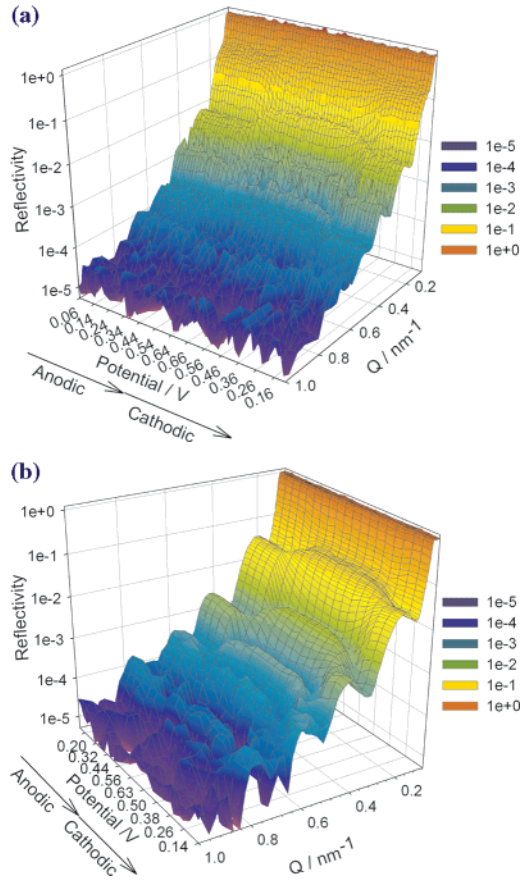

Figure 1. Dynamic NR profiles as functions of Q and E during redox cycling of PVF films exposed to 0.1 M $NaClO_4/D_2O$: (a) $\Gamma = 27$ nmol cm^{-2}, $\upsilon = 10$ mV s^{-1}; (b) $\Gamma = 18$ nmol cm^{-2}, $\upsilon = 1$ mV s^{-1}.

oxidation (reduction) results in fringe compression (expansion); since Q represents inverse space, one is observing film swelling upon oxidation and shrinkage upon reduction. This is chemically reversible on the time scale of a *complete* redox cycle, but on the time scale of the *individual* profiles, swelling occurs over a narrower region of potential than does shrinkage.

The second issue is the extent to which changes in h correlate with electrochemical charge (q). Simplistically, one might view this as equivalent to plots of film mass change, Δm versus q, in an EQCM experiment.[5] However, the complexities of chain and mobile species packing under transient conditions mean that the two are not necessarily equivalent. Figure 2 shows a 3D plot of h and q as functions of E; this is a dynamic compositional map of the system, in which h is dominated by solvent level and q exclusively represents ion content. Two-dimensional $h(Q)$ and $Q(E)$ projections of the 3D compositional vector show that solvation is equilibrated with the redox state, but that the latter is kinetically controlled.

Third, dynamic capability allows exploration of experimental time-scale (here, υ) effects. Analogues of Figure 2 at different scan rates show the interplay of electrochemical and (de)solvation kinetics.

Finally, we seek the transient ion and solvent depth profiles within the film that underlie the simplistic overview of "film thickness". Fuller analyses of $R(Q,E)$ profiles for films bathed in solvent media of different contrast show that the film comprises an interior zone and compositionally distinct interfacial regions near the electrode and the solution. The interior region has spatially uniform composition when the film is fully reduced but has a solvent-rich center when the film is partially oxidized.

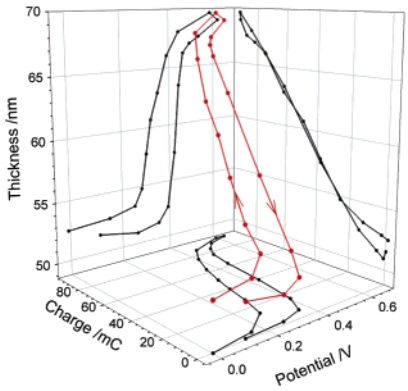

Figure 2. Film thickness and charge as functions of applied potential for the experiment of Figure 1a. Projections: black traces. 3D vector: red trace.

To conclude, in situ NR is now a practical technique for dynamic electrochemical studies. Under dynamic redox switching conditions, PVF films show hysteresis in (de)swelling, incomplete desolvation upon reduction, and transient salt retention under thermodynamically permselective conditions. These effects respond to time scale, manipulated via polymer coverage and potential scan rate. Full analysis will reveal the temporal dependences of polymer, anion, and solvent population depth profiles. This will add a new dimension to the spatially integrated populations available from existing methods and, for the first time, reveal the relationship between individual species populations within the interior of an electroactive film under dynamic conditions.

Acknowledgment. We thank the EPSRC (GR/N00968) for funding, the ILL and ISIS for neutron beam time, and E.L.S. thanks the EPSRC for a studentship.

References

(1) (a) Andria, S. E.; Richardson, J. N.; Kaval, N.; Zudans, I.; Seliskar, C. J.; Heineman, W. R. *Anal. Chem.* **2004**, *76*, 3139−3144. (b) Evans-Kennedy, U.; Clohessy, J.; Cunnane, V. J. *Macromolecules* **2004**, *37*, 3630−3634.
(2) (a) Kolb, D. M. *Angew. Chem.* **2001**, *40*, 1162−1181. (b) Poggi, M. A.; Bottomley, L. A.; Lillehei, P. T. *Anal. Chem.* **2002**, *74*, 2851−2862.
(3) Gardner, J. W.; Bartlett, P. N. *Electronic Noses: Principles and Applications*; Oxford University Press: Oxford, 1999.
(4) Shipway, A. N.; Willner, I. *Acc. Chem. Res.* **2001**, *34*, 421−432.
(5) Hillman, A. R. In *Encyclopaedia of Electrochemistry*; Bard, A. J., Stratmann, M., Eds.; Wiley: New York, 2003; Vol. 3, pp 230−289.
(6) Abruna, H. D.; Denisevich, P.; Umana, M.; Meyer, T. J.; Murray, R. W. *J. Am. Chem. Soc.* **1981**, *103*, 1−5.
(7) Gottesfeld, S. In *Electroanalytical Chemistry*; Bard, A. J., Ed.; Marcel Dekker: New York, 1989; Vol. 15, pp 143−265.
(8) Penfold, J.; Richardson, R. M.; Zarbakhsh, A.; Webster, J. R. P.; Bucknall, D. G.; Rennie, A. R.; Jones, R. A. L.; Cosgrove, T.; Thomas, R. K.; Higgins, J. S.; Fletcher, P. D. I.; Dickinson, E.; Roser, S. J.; McLure, I. A.; Hillman, A. R.; Richards, R. W.; Staples, E. J.; Burgess, A. N.; Simister, E. A.; White, J. W. *J. Chem. Soc., Faraday Trans.* **1997**, *93*, 3899−3917.
(9) Hillman, A. R.; Glidle, A.; Richardson, R. M.; Roser, S. J.; Saville, P. M.; Swann, M. J.; Webster, J. R. P. *J. Am. Chem. Soc.* **1998**, *120*, 12882−12890.
(10) Hillman, A. R.; Bailey, L.; Glidle, A.; Cooper, J. M.; Gadegaard, N.; Webster, J. R. P. *J. Electroanal. Chem.* **2002**, *532*, 269−276.
(11) Saville, P. M.; Gonsalves, M.; Hillman, A. R.; Cubitt, R. *J. Phys. Chem. B* **1997**, *101*, 1−4.
(12) Glidle, A.; Cooper, J.; Hillman, A. R.; Bailey, L.; Jackson, A.; Webster, J. R. P. *Langmuir* **2003**, *19*, 7746−7753.
(13) Glidle, A.; Bailey, L.; Hadyoon, C. S.; Hillman, A. R.; Jackson, A.; Ryder, K. S.; Saville, P. M.; Swann, M. J.; Webster, J. R. P.; Wilson, R. W.; Cooper, J. M. *Anal. Chem.* **2001**, *73*, 5596−5606.
(14) (a) Lipkowski Burgess, I.; Li, M.; Horswell, S. L.; Szymanski, G.; Lipkowski, J.; Majewski, J.; Satija, S. *Biophys. J.* **2004**, *86*, 1763−1776. (b) Burgess, I.; Zamlynny, V.; Szymanski, G.; Schwan, A. L.; Faragher, R. J.; Lipkowski, J.; Majewski, J.; Satija, S. *J. Electroanal. Chem.* **2003**, *550*, 187−199.

JA044682S